Kinetics of the evaporative cooling of an atomic beam

Thierry Lahaye, David Guéry-Odelin

Kinetics of the evaporative cooling of an atomic beam

Thierry Lahaye and David Guéry-Odelin
Laboratoire Kastler Brossel, 24 rue Lhomond, F-75231 Paris Cedex 05, France*
(Dated: January 31, 2006)

We compare two distincts models of evaporative cooling of a magnetically guided atomic beam: a continuous one, consisting in approximating the atomic distribution function by a truncated equilibrium distribution, and a discrete-step one, in which the evaporation process is described in terms of successive steps consisting in a truncation of the distribution followed by rethermalization. Calculations are performed for the semi-linear potential relevant for experiments. We show that it is possible to map one model onto the other, allowing us to infer, for the discrete-step model, the rethermalization kinetics, which turns out to be strongly dependent upon the shape of the confining potential.

PACS numbers: 32.80.Pj,03.75.Pp

I. INTRODUCTION

Evaporative cooling [1] is a very powerful technique that allowed the achievement of quantum degeneracy in dilute atomic vapors [2]. On the theoretical side, apart from direct numerical simulations [3], several models of evaporative cooling have been studied, which can be classified in two categories: *continuous* and *discrete* ones.

In discrete models, the process of evaporative cooling is approximated as a series of truncations of the atomic distribution function, followed by rethermalization towards equilibrium [4]. Through many steps, the phase-space density of the atomic sample increases up to order unity. The advantage of such models lies in their simplicity. However, in the case of trapped clouds of atoms, those models are not realistic, since, experimentally, the evaporation is done by ramping down *continuously* a radio-frequency knife. Moreover, such models give no indication on the kinetics of the evaporation. Therefore, one needs to resort to more elaborated, continuous models, using an appropriate Ansatz for the distribution function, namely a truncated equilibrium function. It is then possible, starting from Boltzmann equation, to obtain the time evolution of the temperature and of the number of atoms [5]. Quantitative comparisons between the predictions of those two types of models have not been made to date.

Evaporative cooling has been revisited in the context of the cooling of a guided atomic beam, in view of achieving a continuous-wave atom laser. The proposal [6] used a continuous evaporation model to predict the possibility of achieving quantum degeneracy by using transverse evaporation on an atomic beam, confined transversally by an harmonic potential. This proposal triggered experimental work in several groups, and a discrete model of the evaporative cooling of a beam was developed [7] in close connection with recent experiments [8, 9].

In this paper, we address the problem of the transverse evaporative cooling of a magnetically guided atomic beam with an energy-selective "knife". We first develop a continuous model using hydrodynamic equations, adapted from [6], for an experimentally realistic transverse potential. Then we describe the same process with a discrete-step evaporation model, analog to the one used in [7]. Finally, we compare the results given by those two distincts models. In particular, this comparison allows us to study the influence of the shape of the confining potential on the kinetics of rethermalization and on the evaporation 'ramp'.

We consider an atomic beam with a flux Φ, a mean longitudinal velocity v, and a temperature T, propagating in a quadrupole magnetic guide of axis z, providing the following semi-linear transverse potential :

$$U(r) = \mu\sqrt{B_0^2 + b^2 r^2} - \mu B_0 \,. \tag{1}$$

Here, μ is the magnetic moment of the atoms, b the transverse gradient of the two-dimensional quadrupole magnetic field created by the guide, $r = \sqrt{x^2+y^2}$ the distance from the guide axis, and B_0 a longitudinal bias field used to avoid Majorana spin-flips [9]. The on-axis potential is taken as the origin of energies. One defines the dimensionless parameter $\alpha \equiv \mu B_0/k_{\rm B}T$. For typical experimental parameters, the evaporation starts with $\alpha \ll 1$ where the potential experienced by the atoms is essentially linear, and degeneracy is reached in the regime $\alpha \gg 1$, where the potential is essentially harmonic. Therefore it is crucial to take into account the real shape of the potential in order to describe the whole evaporation process.

An important quantity characterizing the beam is the s-wave elastic collision rate γ, given by:

$$\gamma = \frac{\sigma}{2\pi^{3/2}} \frac{1+2\alpha}{(1+\alpha)^2} \frac{\Phi}{v} \left(\frac{\mu b}{k_{\rm B}T}\right)^2 \sqrt{\frac{k_{\rm B}T}{m}} \,, \tag{2}$$

where σ is the s-wave scattering cross-section.

Two-dimensional transverse evaporation is applied in order to selectively remove atoms from the beam. In practice, this is achieved by driving transitions to an untrapped state with radio-frequency or microwave fields [9]. The evaporation criterion then relates to the transverse energy ε *and* to the angular momentum of the atom along z. For the sake of simplicity, as in Ref. [5],

we assume in the following that any atom having a transverse energy $\varepsilon \geqslant \eta k_{\rm B}T$, where η is the *evaporation parameter*, is evaporated. This criterion implicitly assumes sufficient ergodicity of the atomic motion. Experimentally, this simple energy criterion can be well approximated by the multi-radii evaporation scheme described in [7].

II. CONTINUOUS MODEL

In this section, we assume that the evaporation takes place over the whole guide length. The height of the energy knife $\varepsilon_{\rm ev}(z) = \eta k_{\rm B}T$ depends on z in order to perform *forced* evaporation. We therefore assume that the beam's distribution function is a local equilibrium one [5], truncated at the energy $\varepsilon_{\rm ev}$.

By using such an Ansatz in the Boltzmann equation, one gets a set of coupled hydrodynamic equations relating the following local quantities characterizing the beam: the linear density $n(z)$, the longitudinal velocity $v(z)$, and the temperature $T(z)$. The details of this somehow lengthy calculation can be found in ref. [6, 10] for the case of a harmonic transverse potential. The validity of such an Ansatz was checked with a molecular dynamics simulation of the process. In the following, we present the generalization of this analytical approach to the case of a semi-linear confinement.

In the stationary regime, the hydrodynamic equations read:

$$\partial_z(nv) = -\Gamma_1 n\,, \tag{3a}$$

$$\partial_z(nv^2 + nv_{\rm th}^2) = -\Gamma_1 nv\,, \tag{3b}$$

$$\partial_z\left[nv\left(\frac{5}{2}v_{\rm th}^2 + \frac{v^2}{2} + \frac{\langle U\rangle}{m}\right)\right] = -n\left(\Gamma_1\frac{v^2}{2} + \Gamma_2 v_{\rm th}^2\right), \tag{3c}$$

where $v_{\rm th} = \sqrt{k_{\rm B}T/m}$. They correspond, respectively, to the evolution of the flux, of the momentum, and of the enthalpy of the beam. The notation $\langle U\rangle$ stands for the thermal average, at the temperature T, of the potential energy U. These equations are well suited to describe a supersonic beam with a high enough Mach number (typically $v \gtrsim 3v_{\rm th}$).

In the semi-linear potential (1), the mean value of the potential energy reads $\langle U\rangle = k_{\rm B}T(2+\alpha)/(1+\alpha)$. Γ_1 and Γ_2 correspond to the evaporation-induced particle and energy loss rates, respectively. They are proportional to the elastic collision rate γ and obviously depend on the evaporation parameter η:

$$\Gamma_i = \gamma\sqrt{\frac{2}{\pi}}\frac{8}{15}K_i(\eta,\alpha) \qquad (i = 1, 2)\,. \tag{4}$$

The functions K_i are given by the following integral:

$$K_i(\eta,\alpha) = \int_0^{\eta+1/2} f(x,\alpha)g_i(x,\eta){\rm d}x, \tag{5}$$

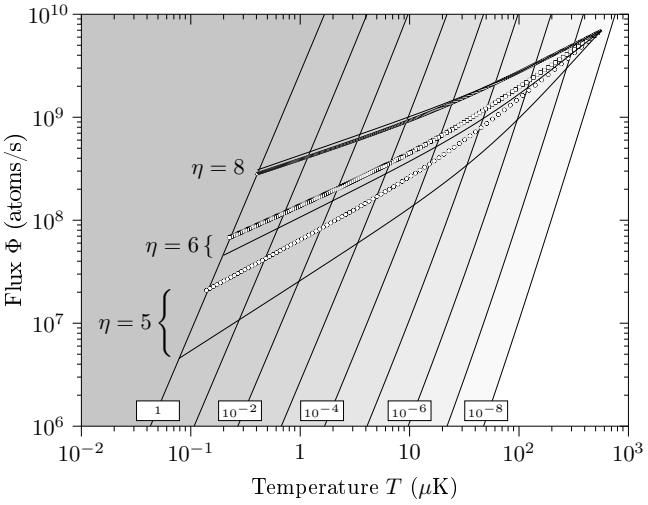

FIG. 1: Evaporation "trajectories" in the temperature/flux plane, for evaporation with a constant η for the continuous model (solid lines) and for the discrete one (dots, each symbol representing the effect of one evaporation step). The background grey scale (with the white labels) shows the on-axis phase-space density. The qualitative shape of those trajectories are similar for both models. For η high enough (e.g., $\eta = 8$), the trajectories are very close in both models. The number of evaporation zones required for reaching degeneracy in the discrete-step model, for $\eta = 5$ (resp. 6, 8), is 88 (resp. 152, 526).

with $f(x,\alpha) = x^{3/2}(5\alpha + 2x){\rm e}^{-\eta-1/2}/(1+2\alpha)$ being a contribution from the density of states per unit length in the semi-linear potential, $g_1(x,\eta) = {\rm e}^{-x}(\eta - x - 1/2) + {\rm e}^{-\eta-1/2}$, and $g_2(x,\eta) = {\rm e}^{-\eta-1/2}(3 + 2\eta - x) + {\rm e}^{-x}[(\eta + 1/2)^2 - 2 - 3x/2 - \eta x]$.

The solid lines in Fig. 1 depict the evolution of the beam's flux and temperature obtained by solving the hydrodynamic equations (3), assuming that the evaporation parameter η remains constant throughout the evaporation. The initial conditions are the experimental ones of Ref. [9], in which ^{87}Rb ($\mu = \mu_{\rm B}/2$) atoms are used: at $z = 0$, one has $\Phi = 7\times10^9$ at/s, $v = 60$ cm/s, and $T = 570$ μK. The gradient is 800 G/cm and a $B_0 = 1$ G bias field is applied. When one increases the value of η, degeneracy (phase-space density $\rho \sim 1$) is achieved for higher fluxes (and therefore higher temperatures) since the evaporated particles are very energetic and consequently the evaporative cooling is more efficient. The change in the slope of the "evaporation trajectories" for $T \sim \mu B_0/k_{\rm B} \sim 30$ μK is due to the fact that the confinement experienced by the atoms changes from essentially linear ($\alpha = 0.06 \ll 1$) to essentially harmonic ($\alpha \gg 1$) as the temperature is reduced. Indeed, the gain in phase-space density scales differently with the shape of the potential [4, 5, 7].

III. DISCRETE-STEP MODEL

We now turn to the description of the evaporative cooling process with a discrete-step model. One evaporation step reduces the atomic flux from Φ to Φ'. After rethermalization, the beam acquires a new temperature T'. In order to calculate the relative variations of flux $\varphi = \Phi'/\Phi$ and of temperature $\tau = T'/T$, we adapt the approach of Ref. [7] to the semi-linear potential and to the energy-dependant evaporation criterion. We therefore introduce the two-dimensional density of states $\varrho(\varepsilon)$ in the semi-linear potential (1): $\varrho(\varepsilon) \propto \varepsilon[2 + \varepsilon/(\mu B_0)]$. The fraction φ of remaining atoms after one evaporation step is:

$$\varphi(\eta,\alpha) = \frac{\int_0^{\eta k_\mathrm{B}T} \varrho(\varepsilon)\,\mathrm{e}^{-\varepsilon/k_\mathrm{B}T}\,\mathrm{d}\varepsilon}{\int_0^{\infty} \varrho(\varepsilon)\,\mathrm{e}^{-\varepsilon/k_\mathrm{B}T}\,\mathrm{d}\varepsilon} \quad (6)$$

$$= 1 - \frac{2 + 2\alpha(1+\eta) + \eta(2+\eta)}{2(1+\alpha)}\,\mathrm{e}^{-\eta}\,. \quad (7)$$

In order to derive τ, we first calculate the transverse energy $\bar{\varepsilon}$ of the remaining atoms:

$$\bar{\varepsilon} = \frac{\int_0^{\eta k_\mathrm{B}T} \varepsilon\,\varrho(\varepsilon)\,\mathrm{e}^{-\varepsilon/k_\mathrm{B}T}\,\mathrm{d}\varepsilon}{\int_0^{\infty} \varrho(\varepsilon)\,\mathrm{e}^{-\varepsilon/k_\mathrm{B}T}\,\mathrm{d}\varepsilon}\,. \quad (8)$$

We define the dimensionless parameter $\theta(\eta,\alpha) \equiv \bar{\varepsilon}/(k_\mathrm{B}T)$ [11]. The conservation of the total energy during rethermalization gives:

$$k_\mathrm{B}T\left(\theta\Phi + \frac{\Phi'}{2}\right) = \Phi'\,\langle U\rangle_{T',\alpha'} + \Phi'\frac{3k_\mathrm{B}T'}{2}\,, \quad (9)$$

where the average $\langle U\rangle_{T',\alpha'}$ of the potential is taken at thermal equilibrium with a temperature T', i.e. with $\alpha' = \alpha/\tau$. This yields a quadratic equation in τ, with the solution:

$$\tau = \frac{2\theta + \varphi - 5\alpha\varphi + \sqrt{28\varphi\alpha(2\theta+\varphi) + (2\theta+\varphi-5\alpha\varphi)^2}}{14\varphi}.$$

One then readily obtains the relative variations of the collision rate γ and of the phase-space density ρ after an evaporation step.

The corresponding "evaporation trajectories" (for η constant) are depicted with circles on Fig. 1. Each symbol represents the flux and temperatures (Φ_n, T_n) of the beam after the n^{th} evaporation zone.

IV. DISCUSSION

We compare the results given by the two models, in terms of evaporation trajectories and of the efficiency of evaporation. As depicted on Fig. 1, the evaporation trajectories have the same qualitative behavior in both models. However, for a given η, the discrete-step evaporation leads to higher final fluxes and temperatures. For a high evaporation parameter ($\eta = 8$), the trajectories given by both models almost coincide.

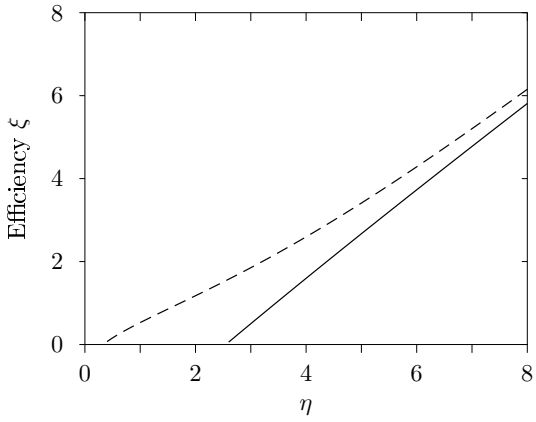

FIG. 2: Evaporation efficiency ξ as a function of the evaporation parameter η, for a harmonic transverse confinement. The solid (resp. dashed) line corresponds to the continuous (resp. discrete-step) evaporation model.

To make these statements more quantitative, we introduce the figure of merit for an evaporative cooling ramp, i.e. the relative variation of the beam's phase-space density ρ for a given loss of particles. We therefore define the evaporation *efficiency* ξ as:

$$\xi \equiv -\frac{\mathrm{d}\ln\rho}{\mathrm{d}\ln\Phi}\,. \quad (10)$$

This quantity is straightforward to calculate for a given evaporation model. Fig. 2 represents $\xi(\eta)$ for the case of a harmonic transverse confinement. As expected, ξ increases with η in both models. It appears that discrete-step evaporation is more efficient than the continuous one, which can be understood qualitatively by the fact that in the latter scheme, some atoms are evaporated without giving rise to a temperature reduction, a process commonly called "spilling" [1, 5]. However, for η high enough, the efficiencies of both models almost coincide.

We now turn to the kinetics of evaporation: for a given shape of the potential (linear or harmonic) and a given value η_D of the evaporation parameter in the discrete model, we determine the corresponding parameter $\eta_C(\eta_D)$ for the continuous model, which leads to the same 'evaporation trajectory' in the (T,Φ) plane. This mapping allows us to extract information on the kinetics aspects of the rethermalization between evaporation zones for the discrete models. More precisely, we infer the number N_c of collisions required to rethermalize between successive zones. For this purpose, we integrate over time the collision rate from the continuous model, with an evaporation parameter $\eta_C(\eta_D)$, between two points (T_n,Φ_n) and (T_{n+1},Φ_{n+1}) of the evaporation trajectory obtained with the discrete model.

To allow for a quantitative comparison between linear and harmonic confinements, we scale the evaporation parameter η_D as in Ref. [4] by defining $\tilde{\eta}_D = \eta_D/2$

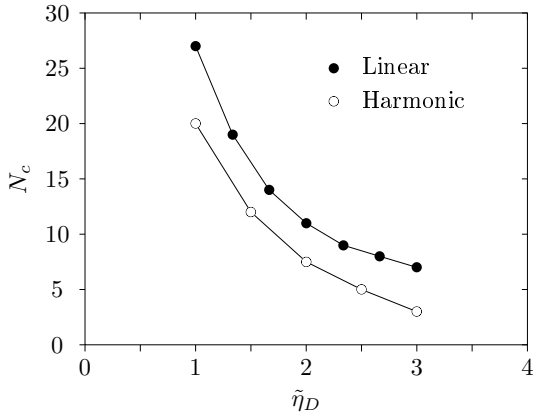

FIG. 3: Number N_c of collisions necessary for rethermalization between two evaporation zones (inferred by mapping the continuous evaporation model onto the discrete one, see text) as a function of the scaled evaporation parameter $\tilde{\eta}_D$. The solid (resp. open) circles correspond to a linear (resp. harmonic) confinement.

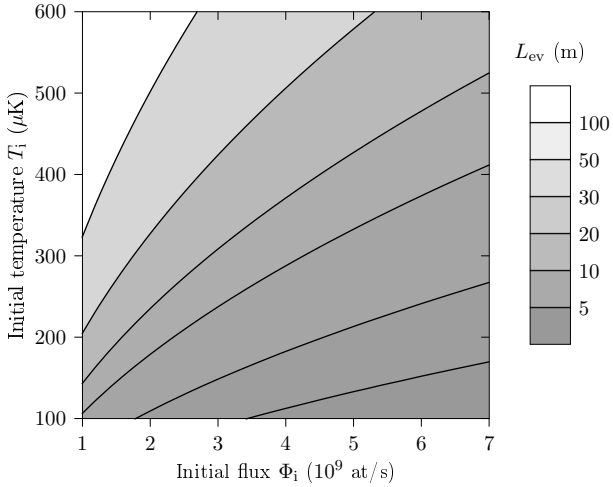

FIG. 4: Minimal evaporation length $L_{\rm ev}$ needed to reach a phase-space density $\rho = 1$ with evaporation at constant η for an atomic beam of initial flux $\Phi_{\rm i}$ and temperature $T_{\rm i}$, propagating at 60 cm/s in a guide with a gradient $b = 800$ G/cm and a longitudinal bias field $B_0 = 1$ G. The iso-contours of $L_{\rm ev}$ show the large advantage of starting with a temperature on the order of 100 μK for reaching degeneracy in a reasonable length. The optimal evaporation parameter η is almost constant ($\simeq 6$) over the whole parameter space explored here.

(resp. $\tilde{\eta}_D = \eta_D/3$) for a harmonic (resp. linear) confinement. Evaporation with a given normalized parameter $\tilde{\eta}_D$ then yields approximately the same flux reduction, independently of the shape of the confining potential. On Fig. 3, we have depicted N_c as a function of $\tilde{\eta}_D$, for both linear and harmonic confinements. As expected, N_c decreases with increasing $\tilde{\eta}_D$, since the atomic distribution is less and less affected by the evaporation, yielding a faster relaxation towards equilibrium. For a linear confinement, 50% to 100% more collisions (as compared to the harmonic one) are required for rethermalization between evaporation zones. This dependence of the kinetics on the shape of the confining potential is reminiscent of what is known for thermalization of confined gas mixtures [12]: the rethermalization time is shorter in a homogeneous system than for a trapped cloud. In a power-law trap of exponent δ, the rethermalization time decreases when δ increases, which simply originates from the different scaling laws of the density of states.

Therefore, two competing effects need to be considered when one studies the whole evaporation process: in a linear potential, the kinetics is slow but the gains in collision rate and in phase-space density scale more favorably [7] than in a harmonic confinement. In terms of the minimum number of collisions required to achieve a given gain in phase-space density, those two effects compensate each other. For instance, we find that at least 500 (resp. 630) collisions are necessary to gain a factor 5×10^7 in phase-space density, in a purely harmonic (resp. linear) potential, for an evaporation parameter $\eta_D \simeq 4.5$ (resp. $\eta_D \simeq 5.5$). However, in terms of evaporation length, the difference between harmonic and linear confinements is still large, as *runaway* evaporation can only occur in the latter case for a two-dimensional evaporation. As an example, we consider two beams with the same initial flux (7×10^9 atoms per second) and temperature (200 μK), with an initial phase-space density $\rho_{\rm i} \simeq 8 \times 10^{-7}$, propagating at 60 cm/s either in a purely harmonic guide, either in a purely linear one. For the former case, the initial collision rate is $\gamma \simeq 37$ s^{-1}, and slightly decreases to $\gamma \simeq 29$ s^{-1} after evaporation to degeneracy. The evaporation is performed at $\eta_C = 6$, a value that minimizes the evaporation length $L_{\rm ev}$, which reaches about 11 m. For a linear confinement, although the initial collision rate is only $\gamma \simeq 19$ s^{-1}, its final value reaches 380 s^{-1} due to the runaway character of the evaporation. The total length needed is only 6 m. Interestingly, the total number of collisions that actually occurred within the beam is almost the same for both confinements (~ 550), as is the evaporation parameter minimizing $L_{\rm ev}$.

In practice, due to Majorana spin-flips [9], the guide potential needs to be semi-linear. For a guide with parameters $b = 800$ G/cm and $B_0 = 1$ G, we have studied the minimal evaporation length $L_{\rm ev}$ needed to reach degeneracy, as a function of the initial flux $\Phi_{\rm i}$ and initial temperature $T_{\rm i}$, assuming a beam velocity of 60 cm/s. The result is plotted on Fig. 4, and shows as expected that $L_{\rm ev}$ decreases with lower $T_{\rm i}$ and higher $\Phi_{\rm i}$. The optimal evaporation parameter is almost constant with the value $\eta = 6$ for our range of parameters $(\Phi_{\rm i}, T_{\rm i})$. The evaporation length determined this way is very well fitted by a function of the form

$$L_{\rm ev} \simeq L_0 \frac{T_{\rm i}^{3/2}}{\Phi_{\rm i}} \,. \qquad (11)$$

This scaling can be easily understood: since here the runaway effect exists only at the very beginning of the

evaporation ramp, before the effective shape of the potential becomes harmonic, the evaporation length is simply inversely proportional to the initial collision rate. For an initial flux 7×10^9 atoms/s, an initial temperature 200 μK, a guide gradient $b = 800$ G/cm and a bias field $B_0 = 1$ G, quantum degeneracy is reached for $L_{\rm ev} \simeq 7$ m, which shows the beneficial influence of the increase of the collision rate at the beginning of the evaporation ramp when the potential is essentially linear.

Actually, the evaporation length deduced here could be reduced by lowering the beam's mean velocity (e.g, with the use of a tilted guide [13]) as it cools down, provided that the beam stays supersonic enough.

Acknowledgments

We are indebted to Jean Dalibard for a careful reading of the manuscript. We thank Johnny Vogels for stimulating discussions at the early stage of this work. We acknowledge fruitful discussions with the ENS laser cooling group, and financial support from the Délégation Générale pour l'Armement.

---

[*] Unité de Recherche de l'Ecole Normale Supérieure et de l'Université Pierre et Marie Curie, associée au CNRS.

[1] W. Ketterle and N. J. Van Druten, Adv. At. Mol. Opt. Phys. **37**, 181 (1996).

[2] M. H. Anderson *et al.*, Science **269**, 198 (1995); K. B. Davis *et al.*, Phys. Rev. Lett. **75**, 3969 (1995).

[3] H. Wu and C. J. Foot, J. Phys. B: At. Mol. Opt. Phys. **29**, L321 (1996).

[4] K. B. Davis, M.-O. Mewes and W. Ketterle, Appl. Phys. B **60**, 155 (1995).

[5] O. J. Luiten, M. W. Reynolds, and J. T. M. Walraven, Phys. Rev. A **53**, 381 (1996).

[6] E. Mandonnet, A. Minguzzi, R. Dum, I. Carusotto, Y. Castin and J. Dalibard, Eur. Phys J. D **10**, 9 (2000).

[7] T. Lahaye and D. Guéry-Odelin, Eur. Phys. J. D **33**, 67 (2005).

[8] T. Lahaye, J. M. Vogels, K. J. Günter, Z. Wang, J. Dalibard, and D. Guéry-Odelin, Phys. Rev. Lett. **93**, 093003 (2004).

[9] T. Lahaye, Z. Wang, G. Reinaudi, S. P. Rath, J. Dalibard and D. Guéry-Odelin, Phys. Rev. A **72**, 033411 (2005).

[10] E. Mandonnet, Ph.D. thesis, Université Paris 6, unpublished (1999).

[11] One finds $\theta(\alpha,\eta) = \{3 + 2\alpha - {\rm e}^{-\eta}[3 + 3\eta + \frac{3}{2}\eta^2 + \frac{1}{2}\eta^3 + \alpha(2 + 2\eta + \eta^2)]\}/(1+\alpha)$.

[12] M. Anderlini and D. Guéry-Odelin, to appear in Phys. Rev. A, `cond-mat/0507681`.

[13] T. Lahaye, P. Cren, C. Roos and D. Guéry-Odelin, Commun. Nonlinear Sci. Numer. Simul. **8**, 315 (2003).